

Upper limit for the cross-section of the overlapping scalar resonances $f_0(980)$ and $a_0(980)$ produced in proton–proton collisions in the range of the reaction threshold

This article has been downloaded from IOPscience. Please scroll down to see the full text article.

2003 J. Phys. G: Nucl. Part. Phys. 29 2235

(<http://iopscience.iop.org/0954-3899/29/9/317>)

[The Table of Contents](#) and [more related content](#) is available

Download details:

IP Address: 149.156.90.110

The article was downloaded on 10/01/2010 at 14:14

Please note that [terms and conditions apply](#).

Upper limit for the cross-section of the overlapping scalar resonances $f_0(980)$ and $a_0(980)$ produced in proton–proton collisions in the range of the reaction threshold

P Moskal^{1,2}, H-H Adam³, A Budzanowski⁴, R Czyżykiewicz²,
D Grzonka¹, M Janusz², L Jarczyk², B Kamys², A Khoukaz³, K Kilian¹,
C Kolf¹, P Kowina^{1,5}, T Lister³, W Oelert¹, C Piskor-Ignatowicz²,
J Przerwa², C Quentmeier³, T Rożek^{1,5}, R Santo³, G Schepers¹,
T Sefzick¹, M Siemaszko⁵, J Smyrski², A Strzałkowski², A Täschner³,
P Winter¹, M Wolke^{1,7}, P Wüstner⁶ and W Zipper⁵

¹ IKP, Forschungszentrum Jülich, D-52425 Jülich, Germany

² Institute of Physics, Jagellonian University, PL-30-059 Cracow, Poland

³ IKP, Westfälische Wilhelms-Universität, D-48149 Münster, Germany

⁴ Institute of Nuclear Physics, PL-31-342 Cracow, Poland

⁵ Institute of Physics, University of Silesia, PL-40-007 Katowice, Poland

⁶ ZEL, Forschungszentrum Jülich, D-52425 Jülich, Germany

E-mail: p.moskal@fz-juelich.de

Received 5 June 2003

Published 4 August 2003

Online at stacks.iop.org/JPhysG/29/2235

Abstract

Utilizing a missing mass technique we investigate the $pp \rightarrow ppX$ reaction scanning beam energies in the range permitting to create a mass close to that of the $f_0(980)$ and $a_0(980)$ scalar resonances, but still below the K^+K^- threshold where they decay dominantly into $\pi\pi$ and $\pi\eta$ mesons, respectively. Prior to the data analysis we introduce a notion of the close to threshold total cross-section for broad resonances. We estimated for the overlapping mesons a_0 and f_0 the total cross-section to be smaller than 430 nb at excess energy of $Q = 5$ MeV. The experiment has been performed at the Cooler Synchrotron (COSY) using the COSY-11 facility.

1. Introduction

A study of the 1 GeV/ c^2 mass range is motivated by the continuing discussion on the nature of the scalar resonances $f_0(980)$ and $a_0(980)$, which have been interpreted as exotic four quark states [1], conventional $q\bar{q}$ states [2, 3] or molecular such as $K\bar{K}$ bound state [4, 5].

⁷ Present address: The Svedberg Laboratory, Thunbergsvägen 5A, Box 533, S-75121 Uppsala, Sweden.

Within the framework of the Jülich meson exchange model for $\pi\pi$ [6] and $\pi\eta$ scattering, the $K\bar{K}$ interaction dominated by vector meson exchange gives rise to a $K\bar{K}$ bound state identified with the $f_0(980)$ in the isoscalar sector, while the isovector $a_0(980)$ is concluded to be a dynamically generated threshold effect [7, 8]. Both shape and absolute scale of $\pi\pi \rightarrow K\bar{K}$ transitions turn out to depend crucially on the strength of the $K\bar{K}$ interaction, which, in turn is prerequisite of a $K\bar{K}$ bound state interpretation of the $f_0(980)$. Although the $K\bar{K}$ decay mode of $f_0(980)$ and $a_0(980)$ is rather weak in comparison to the dominant $\pi\pi$ and $\pi\eta$ decay channels [9], even a new theoretical analysis based on the chiral approach cannot account for the $f_0(980)$ and $a_0(980)$ if the $K\bar{K}$ channel is not introduced additionally to the $\pi\pi$ and $\pi\eta$ interaction [10]. An analysis of the $\pi\pi$ and $K\bar{K}$ interaction [11] showed that f_0 corresponds to poles of three Riemann–Sheetz which appears physically as an object with a decay width of about 400 MeV and a narrow peak width of about 50 MeV. The same parameters of the f_0 were found by utilizing a unitarized quark model, according to which f_0 was interpreted as a $q\bar{q}$ state with a large admixture of $K\bar{K}$ virtual state [12]. The origin of the scalar resonances was also thoroughly studied by means of a coupled channel analysis considering $\pi\pi$, $K\bar{K}$ and $\sigma\sigma$ meson–meson scattering [13, 14]. Decreasing gradually the interchannel coupling constants, it was inferred that for some solutions the f_0 corresponds to the $K\bar{K}$ bound state [14, 15] at the limit of the fully uncoupled case.

In high-energy experiments, the f_0 meson is observed as a resonance in the system of two pions produced in the variety of hadro-production reactions [16–19] or in hadronic decays of heavier mesons [20–22] or the Z^0 boson [23, 24]. These experiments study invariant masses of the created neutral ($\pi^0\pi^0$) [16, 18, 22] and charged ($\pi^+\pi^-$) [17, 19–21, 23]) pion pairs. Similarly, charged [25, 26] and neutral a_0 [27] mesons were observed as a clear signal in an invariant mass spectrum of the $\eta\pi$ system.

Complementary to these approaches, which studied the interaction of $\pi\pi$, $K\bar{K}$ and $\pi\eta$ meson pairs, we investigate the possible manifestation of the mesons f_0 and/or a_0 as ‘doorway states’ leading to meson production in proton–proton collisions, namely $pp \rightarrow pp f_0(a_0) \rightarrow pp$ mesons. By measuring the missing mass with respect to the pp -system we study the f_0 – a_0 system as a genuine particle produced in the proton–proton collisions. In section 3 we report of the first experimental investigation, which concerns the close to threshold production of the broad neutral resonances via proton–proton collisions in the 1 GeV/ c^2 mass range. Moreover, we have studied the f_0 and a_0 mass range below the $K\bar{K}$ threshold, where they can decay into non-strange mesons only.

It is obvious that for the excitation of a broad resonance the phrase ‘close to threshold’ is not well defined and implies here that the beam momentum is such that masses just in the range of the resonance can be excited. This issue will be discussed in section 2.

In a recent publication [28], the COSY-11 collaboration presented data on the close-to-threshold K^+K^- production following the proton–proton interaction at the excess energy of $Q = 17$ MeV. The obtained distribution of the missing mass to the p – p system is shown in figure 1. The Monte-Carlo simulations demonstrate that the non-resonant K^+K^- production (solid line) is hardly distinguishable from the resonant $pp \rightarrow pp f_0(980) \rightarrow pp K^+K^-$ reaction sequence (dashed line) [29]. In fact, the statistics of the data was not sufficient to favour one of the two processes. The issue whether there is a chance to distinguish between $K\bar{K}$ pairs originating from the decay of genuine f_0/a_0 resonance and those produced by strong $\pi\pi$ – $K\bar{K}$ correlation is at present under theoretical investigation [8].

Since there exists no experimental information of the close to threshold total cross-section for the production of the f_0 and a_0 mesons⁸, before the presentation of the COSY-11

⁸ Recently the ANKE collaboration reported results on the close-to-threshold production of the a_0^+ meson via the $pp \rightarrow d K^+ \bar{K}^0$ reaction [42, 43].

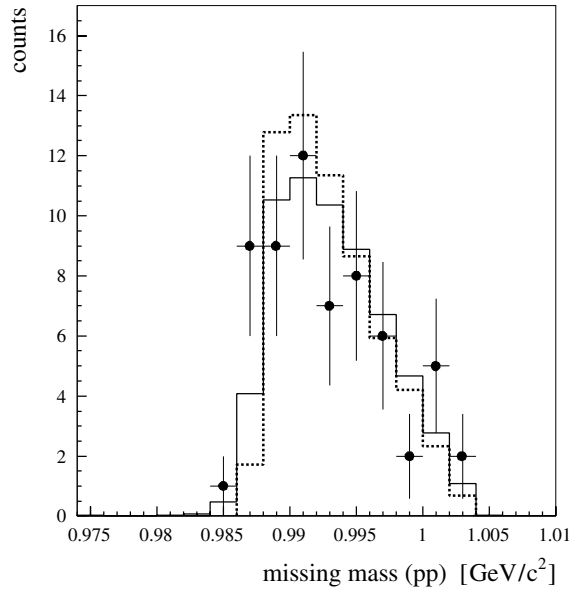


Figure 1. Experimental spectrum of the K^+K^- invariant mass measured for the reaction $pp \rightarrow ppK^+K^-$ at a beam momentum of 3.356 GeV/c (data points). The width of the bins corresponds to the experimental resolution of the mass determination (FWHM \approx 2 MeV). Solid and dashed lines show the Monte-Carlo simulations under the assumption of the direct and resonance production, correspondingly [29].

measurement, we will estimate an expected order of magnitude for the considered values at the excess energy of $Q = 5$ MeV at which theoretical predictions for the K^+K^- production are available [30]. The calculation, based upon the one-pion exchange model and the Breit–Wigner prescription for the f_0 resonance, shows that the production of a $K\bar{K}$ pair through the f_0 resonance ($pp \rightarrow pp f_0(980) \rightarrow pp K^+K^-$) contributes at $Q = 5$ MeV, with respect to the K^+K^- threshold, by a factor of at least 20 less than the non-resonant creation. Extrapolating the measured cross-sections of the $pp \rightarrow pp K^+K^-$ reaction [28, 31] to $Q = 5$ MeV, one obtains the value of 0.08 nb. Thus combining the above information and additionally taking into account that the branching ratio of f_0 meson decay into K^+K^- is about 2% [30], one expects that very close to threshold at $Q = 5$ MeV (with respect to the $pp K^+K^-$ final state), the f_0 meson should be produced with a cross-section in the order of $0.08 \text{ nb} * 50/20 = 0.2 \text{ nb}$. However, the branching ratio of f_0 that decay into $K\bar{K}$ pairs is not well established [9] and may be much smaller than the above assumed value of 2%. Naively one would expect it to be very small, since due to the energy conservation only a few per cent of the resonance can decay into strange particles and moreover only a fraction of that part will decay into a K^+K^- pair.

In case of the $NN \rightarrow NN a_0$ reaction, the total cross-section was estimated using an effective Lagrangian approach taking into account the one-pion exchange mechanism and the production via t-channel exchanges with $\pi\eta$ and πf_1 mesons [32]. The assumption of the positive interference between s- and u-channel of the one-pion exchange results in the value of about 20 nb at $Q = 5$ MeV; however, an exchange of heavier mesons was not taken into account. In addition it should be noted that a different choice of coupling constants and cut-off parameter $\Lambda_{\pi NN}$ would easily change the expected cross-section by a factor of five in either direction.

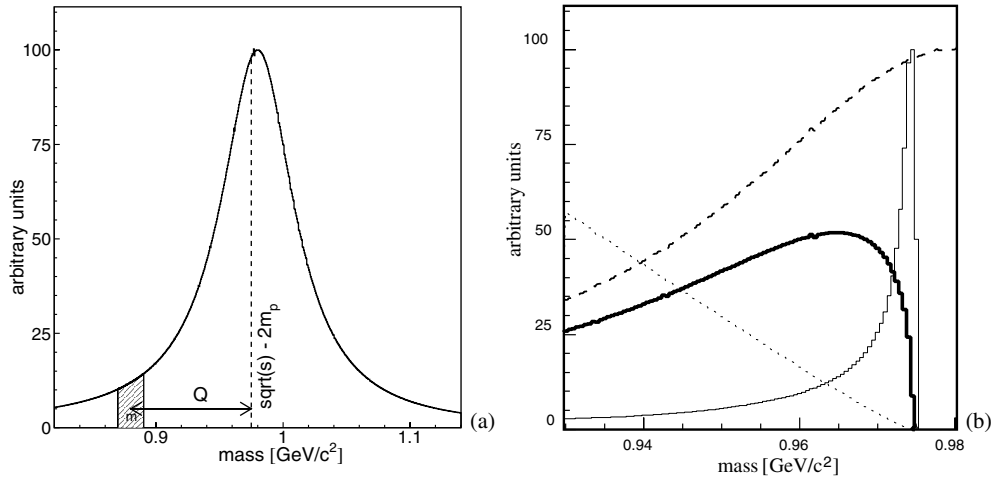


Figure 2. (a) Breit-Wigner distribution with a mean value of $m_0 = 980 \text{ MeV}/c^2$ and a width $\Gamma = 70 \text{ MeV}/c^2$. If the measurement would be performed with the \sqrt{s} as depicted by the dashed line then the mass m would be measured with the centre-of-mass excess energy equal to Q . (b) *Simulations*: horizontal axis denotes the mass of the produced system X via the $pp \rightarrow ppX$ reaction. Long-dashed line denotes a fraction of the Breit-Wigner distribution, as shown in figure 2(a). Thin-solid line represents the efficiency of the COSY-11 detection system for the simultaneous detection of the two outgoing protons from the $pp \rightarrow ppX$ reaction. Short-dashed line shows the decrease of the phase space volume with the increase of the created mass. The phase space volume was weighted by the proton-proton FSI enhancement factor taken from [34]. The thick-solid line results as a convolution of the above described distributions.

The above appraisal indicates that at a few MeV above the production threshold a total cross-section for the $pp \rightarrow pp a_0(f_0)$ reactions is expected to be of the order of 1 nb to 100 nb.

2. Definition of the close-to-threshold total cross-section for a broad resonance

The study of short-living (broad) particles in the $pp \rightarrow ppX$ reaction requires special care [33] when the energy at the centre of mass is close to the sum of the masses of the two protons and the average mass of the meson. As already mentioned due to the broad mass distribution of such particles the notion of the reaction threshold is not well defined. It is naturally a matter of scale whether a given resonance is considered as a broad one. Experimentally, by a broad resonance we define a particle with its full width Γ at half maximum of the mass distribution (spectral function) being much larger than the experimental accuracy of the mass determination, or with a such broad width that the acceptance of the detection system changes significantly over the resonance mass range. Both criteria apply for the measurements performed and discussed in the present contribution.

In the following we will propose a definition of the total cross-section as a function of the excess energy $Q = \sqrt{s} - 2 \cdot m_p - m_X$, which is valid also when Q is small compared to the width Γ of the produced meson.

Performing the measurement with the total centre-of-mass energy \sqrt{s} close to the sum of the average mass of the particles in the exit channel, different mass ranges of the broad particle are populated with different excess energies: $Q(m) = \sqrt{s} - (2 \cdot m_p + m)$ (see figure 2(a)). This implies that the observed mass distribution appears to be different from the one which

would be determined at an excess energy much larger than the width of the broad meson. Neglecting dynamical effects, in case of large \sqrt{s} the mass distribution can be roughly approximated by the Breit–Wigner function, as shown in figure 2(a).

The measurements of the $pp \rightarrow ppX$ reactions, reported here, have been performed by means of the COSY-11 detection system [35]. The thick solid line in figure 2(b) shows the expected missing mass distribution simulated for the total centre-of-mass energy \sqrt{s} equivalent to a maximal produced mass ($\sqrt{s} - 2m_p$) smaller than the average mass of the simulated meson. The shape of this curve results from convoluting the meson spectral density (long-dashed line) with both (i) the decrease of the phase space volume with decreasing excess energy Q weighted by the proton–proton FSI enhancement factor (short-dashed line) and with (ii) the efficiency of the COSY-11 detection system for the simultaneous registration of the two outgoing protons from the $pp \rightarrow ppX$ reaction (thin solid line).

The number of observed events per mass bin $\frac{dN}{dm}$ can be written as

$$\frac{dN}{dm}(m, Q) = \frac{d\sigma}{dm}(m, Q) \cdot L \cdot E_{ff}(Q), \quad (1)$$

with L and E_{ff} denoting the integrated luminosity and the efficiency of the COSY-11 detection system, respectively. As proved by the extensive Monte-Carlo simulations, the COSY-11 efficiency is in a good approximation independent of the produced mass and depends on the excess energy Q only. The cross-section $\frac{d\sigma}{dm}$ for the creation of a mass m is expressed by

$$\frac{d\sigma}{dm}(m, Q) = |M(Q)|^2 \cdot V_{ps}(Q) \cdot \text{FSI}_{pp}(Q) \cdot \text{SD}(m, m_0, \Gamma) \quad (2)$$

$$\frac{d\sigma}{dm}(m, Q) = \sigma_{\text{primary}}(Q) \cdot \text{SD}(m, m_0, \Gamma), \quad (3)$$

where $M(Q)$ stands for the matrix element accounting for the production mechanism, and the last term SD denotes the spectral density of the produced meson with the average mass and width equal to m_0 and Γ , respectively. The $V_{ps}(Q)$ and $\text{FSI}_{pp}(Q)$ represent the phase space volume available to the outgoing particles and the proton–proton FSI enhancement factor, respectively [36]. The term $\sigma_{\text{primary}}(Q)$ combines all excess energy-dependent factors and could be referred to as a primary production cross-section of producing a mass bin of the resonance which is by a value of Q smaller than the maximum kinematically available mass. It should be noted that all factors in equations (1) and (2) depend on the excess energy Q only, except the spectral density which is a function of the created mass m . This means that the number of events per mass bin can be expressed as follows:

$$\frac{dN}{dm}(m = \sqrt{s} - 2m_p - Q, Q) = \text{constant}(Q) \cdot \text{SD}(m, m_0, \Gamma). \quad (4)$$

Scanning the resonance experimentally by changing the value of $\sqrt{s} = 2m_p + m + Q$ and keeping in the analysis a constant value of Q allows to reproduce the mass distribution of the created meson, even without knowing exactly the energy dependence of the detection efficiency and other factors. Note that if $\sqrt{s} - 2m_p$ is within the range of the broad resonance (see figure 2(a)) then not all parts of the resonance can be created. Thus, it is not trivial from such a single measurement how to extract the total cross-section. However, by scanning the resonance with different values of $\sqrt{s} - 2m_p$ one can define the total cross-section at a given excess energy Q as an integral over the whole resonance region of the differential cross-section $\frac{d\sigma}{dm}(m, Q)$ keeping in the integration Q as a constant, thus

$$\sigma(Q) = \int_{2m_p}^{\infty} \frac{d\sigma}{dm}(m = \sqrt{s} - 2m_p - Q, Q) d\sqrt{s}. \quad (5)$$

Table 1. Result of the analysis of the $pp \rightarrow ppX$ reaction measured at COSY-11; Δ is defined in equation (10).

Beam momentum (MeV/c)	Maximum mass of X (MeV/c ²)	Δ (nb)	Error (Δ) (nb)
3214.0	959.6	0.0	0.0
3226.6	963.6	11.3	5.6
3232.1	965.4	7.7	5.3
3238.0	967.2	19.3	5.8
3242.9	968.8	13.6	5.3
3253.1	972.0	23.1	5.7
3282.9	981.4	15.1	4.9

Please note that if the spectral density function is normalized to unity then $\sigma(Q)$ is directly equal to the primary cross-section $\sigma_{\text{primary}}(Q)$. This can be inferred by substituting equations (3) in (5).

Assuming that similar to the production process for pseudoscalar mesons the value of $|M|^2$ will be constant with small values of Q [36, 37], one expects that the energy dependence of $\sigma(Q)$ from equation (5) will be determined by the Q -dependence of the phase space and the dominant proton–proton FSI.

3. Measurement of the $pp \rightarrow ppX$ reaction close-to-threshold for the production of f_0 and a_0 mesons

In the following we will present the analysis of the measurements which were primordially devoted to production studies of the η' meson in proton–proton collisions [38]. The experiment was performed at seven different beam momenta (listed in table 1). The maximum mass ($\sqrt{s} - 2m_p$) available in these experiments covered a range from 959.6 MeV/c² to 981.4 MeV/c². This is the region below and close to the average mass of the $f_0(980)$ and $a_0(980)$ masses, and hence the signal from the production of these mesons should indeed influence the overall observed missing mass spectra. Figure 3 presents one of the missing mass distributions extracted from the experimental data taken at a total centre-of-mass energy equivalent to the maximum created mass of $M = 972$ MeV/c².

Certainly the shape of the ‘background’ below the clear η' peak differs from the shape of the missing mass distribution (thick solid line in figure 2(b)) simulated for the Breit–Wigner resonance. This is due to the fact that the experimental missing mass spectrum comprises also contributions from non-resonant multi-pion, $\pi\eta$ and $\pi\omega$ production. Thus, taking also into account the well-known yield originating from the η' production, one can generally extend equation (4) to

$$\frac{dN}{dm}(m, Q) = \text{constant}(Q) \cdot \text{SD}(m, m_0, \Gamma) + \frac{dN}{dm}(\text{multi-}\pi, \pi\eta, \pi\omega, \sqrt{s}) + \frac{dN}{dm}(\eta', \sqrt{s}). \quad (6)$$

A mass bin corresponding to $Q = 5 \text{ MeV} \pm \Delta Q$ with $\Delta Q = 5 \text{ MeV}$ was chosen in the analysis for each of the seven measurements under investigation (see as an example the shaded area in figure 3). The number of events per this mass bin has been calculated for seven measurements, and after the correction for the detection efficiency has been normalized to the corresponding

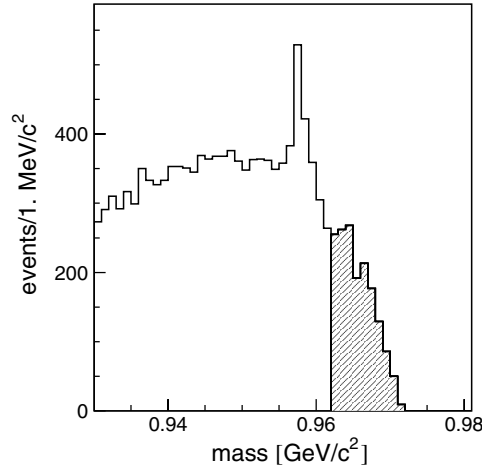


Figure 3. *Experiment:* missing mass distribution is determined for the $pp \rightarrow ppX$ reaction at 14 MeV excess energy above the threshold for the η' meson production [38]. The peak at 958 MeV/ c^2 corresponds to the production of the η' meson. The shaded area denotes the part of the spectrum used in the present analysis.

integrated luminosity:

$$\begin{aligned} \Delta N(\sqrt{s}) &= \frac{1}{L} \int_{Q=0 \text{ MeV}}^{Q=10 \text{ MeV}} \frac{dN}{dm} \frac{1}{E_{ff}(Q)} dm \\ &= \int_{Q=0 \text{ MeV}}^{Q=10 \text{ MeV}} \sigma_{\text{primary}} \cdot \text{SD}(\sqrt{s} - 2m_p - Q, m_0, \Gamma) dm \\ &\quad + \int_{Q=0 \text{ MeV}}^{Q=10 \text{ MeV}} \left(\frac{d\sigma}{dm}(\text{multi-}\pi, \pi\eta, \pi\omega, \sqrt{s}) + \frac{d\sigma}{dm}(\eta', \sqrt{s}) \right) dm. \end{aligned} \quad (7)$$

Simulated distributions for the case of the direct 2π and 3π creations are shown in figure 4. One can observe that their shapes differ (i) from each other and (ii) again from the one determined experimentally. The latter discrepancy can be attributed at least qualitatively to contributions of the productions of the $f_0(980)$ and/or $a_0(980)$ mesons to the experimental spectrum.

Subsequently, if necessary, the well-known values of $\frac{d\sigma}{dm}(\eta', \sqrt{s})$ [38] were subtracted from the above defined $\Delta N(\sqrt{s})$:

$$\Delta N'(\sqrt{s}) = \Delta N(\sqrt{s}) - \int_{Q=0 \text{ MeV}}^{Q=10 \text{ MeV}} \frac{d\sigma}{dm}(\eta', \sqrt{s}) dm. \quad (8)$$

Further, in order to account for the contribution from the multi-pion, $\pi\eta$ and $\pi\omega$ production we subtracted from each $\Delta N'(\sqrt{s})$ the value determined for the lowest measured energy. The result is shown in figure 5(a), where the variable Δ at the vertical axis reads

$$\Delta = \Delta N'(\sqrt{s}) - \Delta N'(\sqrt{s}_{\text{lowest}}) = 2 \cdot m_p + 959.6 \text{ MeV}. \quad (9)$$

On the other hand, assuming changes of the cross-section for the non-resonant multi-pion $\pi\eta$ and $\pi\omega$ production to be negligible, the value of Δ can be expressed as follows:

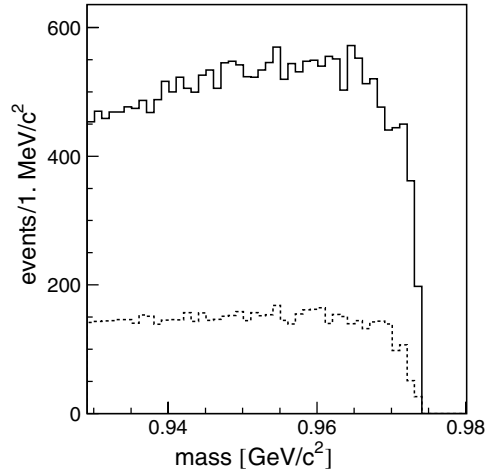


Figure 4. Simulations: missing mass distributions for the reactions $pp \rightarrow pp2\pi$ (dashed line) and $pp \rightarrow pp3\pi$ (solid line). Please note that the shape of these spectra differ from each other and both are different from the missing mass distribution shown in figure 2(b).

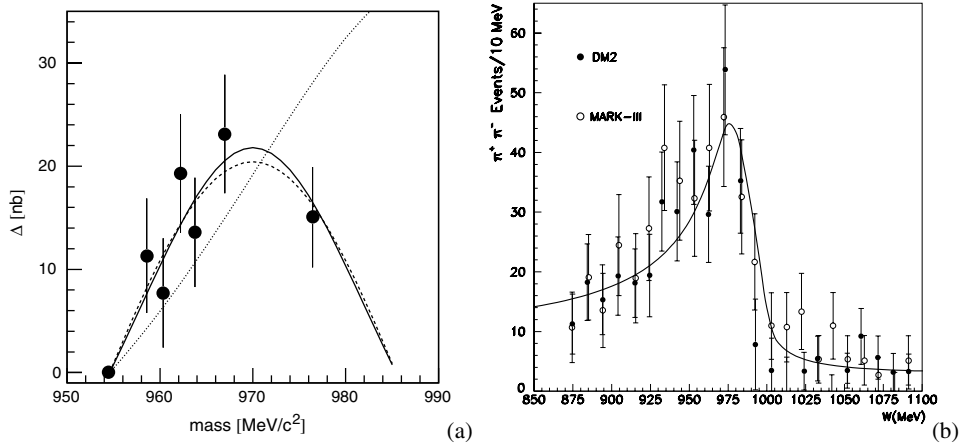


Figure 5. (a) Points denote number of events, measured for the 10 MeV upper bin of the missing mass spectrum for the $pp \rightarrow ppX$ reaction, as depicted by the shaded area in figure 3, normalized to the integrated luminosity. The value obtained at $959.6 \text{ MeV}/c^2$ was subtracted from each point. The x -axis denotes the mass corresponding to $Q = 5 \text{ MeV}$. For example, the point corresponding to the spectrum of figure 3 ($\sqrt{s} - 2m_p = 972 \text{ MeV}$) is plotted at a mass value of $967 \text{ MeV}/c^2$. Lines show the result of simulations of the $pp \rightarrow ppX$ reaction, with X being the Breit–Wigner type meson resonance of the following parameters: (dotted line) mass $990 \text{ MeV}/c^2$, width $65 \text{ MeV}/c^2$ and $\sigma_{\text{primary}} = 750 \text{ nb}$; (solid line) mass $970 \text{ MeV}/c^2$, width $40 \text{ MeV}/c^2$ and $\sigma_{\text{primary}} = 400 \text{ nb}$; (dashed line) mass $970 \text{ MeV}/c^2$, width $65 \text{ MeV}/c^2$ and $\sigma_{\text{primary}} = 1200 \text{ nb}$. (b) $\pi^+\pi^-$ event distribution in the $J/\Psi \rightarrow \phi\pi^+\pi^-$ decay around the f_0 mass. Data were taken by DM2 [39] and MARK-III [40] collaborations. Solid line depicts the result of the calculations of [41].

$$\Delta = \sigma_{\text{primary}} \cdot \int_{Q=0 \text{ MeV}}^{Q=10 \text{ MeV}} \text{SD}(m, \sqrt{s} - 2m_p - Q, \Gamma) dm - \sigma_{\text{primary}} \cdot \int_{Q=0 \text{ MeV}}^{Q=10 \text{ MeV}} \text{SD}(m, \sqrt{s}_{\text{lowest}} - 2m_p - Q, \Gamma) dm. \quad (10)$$

Values determined for Δ are given in table 1 and also shown in figure 5(a).

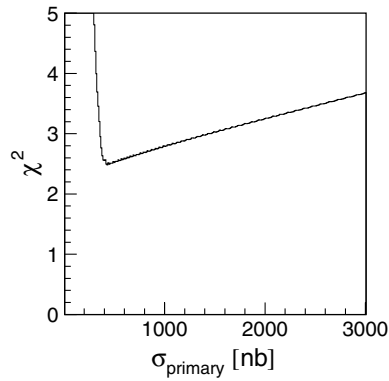


Figure 6. χ^2 as a function of the total cross-section. Number of degrees of freedom is equal to 3.

The curves in this figure represent calculations performed according to equation (10) approximating the spectral function $SD(m, m_0, \Gamma)$ by the Breit–Wigner distribution. The obtained result demonstrates that the data are sensitive to the average mass of the created meson or mesons but rather non-sensitive to the width of an assumed Breit–Wigner structure. The latest volume of the *Review of Particle Physics* [9] shows that the parameters for $f_0(980)$ and $a_0(980)$ mesons are very similar to each other:

$$\begin{aligned} f_0(980): \quad m &= 980 \pm 10 \text{ MeV}, & \Gamma &= 40 \text{ to } 100 \text{ MeV} \\ a_0(980): \quad m &= 984.7 \pm 1.2 \text{ MeV}, & \Gamma &= 50 \text{ to } 100 \text{ MeV} \end{aligned}$$

and therefore we cannot distinguish between these two resonances in a missing mass analysis from the proton–proton interaction.

A fit to the resonance-like structure of figure 5(a) results in values of $m_0 = 969^{+3}_{-2}$ MeV and $\sigma_{\text{primary}} = 430^{+2070}_{-100}$ nb and is nearly identical to the solid line in figure 5(a). The quality of the fit can be estimated from the χ^2 distribution shown in figure 6. It is worth to note that the obtained structure is in line with the measurements of the $\pi^+\pi^-$ invariant mass distribution of the J/Ψ decay into $\phi\pi^+\pi^-$ system as shown in figure 5(b). It is rather well justified that the total cross-section of multi-pion and $\pi\eta$ changes only insignificantly over the studied 22 MeV excess energy range since the present measurements were performed some 560 MeV and 300 MeV above the 3π and $\pi\eta$ thresholds. Still, it cannot be excluded that the variations of Δ are due to the growth of an unknown cross-section for $\pi\omega$ production since in this case the excess energy changes from 42 to 64 MeV. Therefore, the determined value of the total cross-sections for a_0/f_0 resonances can only be treated as an upper limit.

4. Conclusion

For the example of the production of the $f_0(980)$ and/or $a_0(980)$ mesons, we discuss the notion of the reaction threshold in case of broad resonances where the available phase space volume for a given mass bin changes significantly. Ansatz of equation (2) leads to a simple definition of the differential and total cross-section also in the case of the close-to-threshold production of a broad resonance.

The performed measurements of the $pp \rightarrow ppX$ reaction at seven beam momenta close to the threshold of f_0 and a_0 mesons revealed an enhancement in the missing mass spectrum. If the observed structure were due to the production of the object possessing the Breit–Wigner form, its total cross-section introduced in equation (5) would be equal to about 430 nb at excess

energy of $Q = 5$ MeV. However, due to the unknown influence of the $\pi\omega$ production, we can treat this value only as an estimation of an upper limit for the production of f_0 and a_0 meson via the $pp \rightarrow ppX$ reaction. Here we would like to stress that this is the first experimental investigation utilizing a missing mass techniques of the production of these scalar resonances close to the kinematical threshold. The determined upper limit of the total cross-section is much larger than expected from existing theoretical estimations, which however take into account only a part of the possible production mechanisms. In case of f_0 , for example, one could consider also a production via an excitation of baryonic resonances. Particle Data Group (PDG) [9] reports a few N^* resonances around 1700 MeV with widths of 50–250 MeV, which decay predominantly into the $N\pi\pi$ channel.

Acknowledgments

We would like to thank J A Oller for comments to the first version of the manuscript. The work has been partly supported by the European Community-access to research infrastructure action of the improving human potential programme as well as the International Büro and the Verbundforschung of the BMBF.

References

- [1] Jaffe R 1977 *Phys. Rev. D* **15** 267
- [2] Morgan D and Pennington M R 1993 *Phys. Rev. D* **48** 1185
- [3] Kleefeld F *et al* 2002 *Phys. Rev. D* **66** 034007
- [4] Weinstein J and Isgur N 1990 *Phys. Rev. D* **41** 2236
- [5] Wang Z S *et al* 2000 *Nucl. Phys. A* **684** 429c
- [6] Lohse D *et al* 1990 *Nucl. Phys. A* **516** 513
- [7] Krehl O *et al* 1997 *Phys. Lett. B* **390** 23
- [8] Haidenbauer J 2002 *Proc. Symp. on Threshold Meson Production in pp and pd Interaction (Cracow, Poland, 20–24 June 2001)* ed P Moskal and M Wolke *Schriften des FZ-Jülich Matter Mater.* **11** 225 (webpage: <http://ikpe1101.ikp.kfa-juelich.de/>)
- [9] Hagiwara K *et al* 2002 *Phys. Rev. D* **66** 010001
- [10] Oller J A *et al* 1999 *Phys. Rev. D* **59** 074001
- [11] Zou B S and Bugg D V 1993 *Phys. Rev. D* **48** R3948
- [12] Törnqvist N A 1982 *Phys. Rev. Lett.* **49** 624
- [13] Kamiński R *et al* 1997 *Phys. Lett. B* **413** 130
- [14] Kamiński R *et al* 1999 *Eur. Phys. J. C* **9** 141
- [15] Kamiński R *et al* 2000 *Acta. Phys. Pol. B* **31** 2467
- [16] Alde D *et al* 1995 *Z. Phys. C* **66** 375
Alde D *et al* 1997 *Phys. Lett. B* **397** 350
Alde D *et al* 1998 *Eur. Phys. J. A* **3** 361
- [17] Barberis D *et al* 1999 *Phys. Lett. B* **462** 462
- [18] Barberis D *et al* 1999 *Phys. Lett. B* **453** 325
- [19] Breakstone A *et al* 1986 *Z. Phys. C* **31** 185
- [20] Aitala E M *et al* 2001 *Phys. Rev. Lett.* **86** 765
Aitala E M *et al* 2001 *Phys. Rev. Lett.* **86** 770
- [21] Akhmetshin R R *et al* 1999 *Phys. Lett. B* **462** 371
- [22] Akhmetshin R R *et al* 1999 *Phys. Lett. B* **462** 380
- [23] Ackerstaff K *et al* 1998 *Eur. Phys. J. C* **4** 19
- [24] Abreu P *et al* 1999 *Phys. Lett. B* **449** 364
- [25] Ackerstaff K *et al* 1998 *Eur. Phys. J. C* **5** 411
- [26] Gay J B *et al* 1976 *Phys. Lett. B* **63** 220
- [27] Teige S *et al* 1998 *Phys. Rev. D* **59** 012001
- [28] Quentmeier C *et al* 2001 *Phys. Lett. B* **515** 276
- [29] Quentmeier C 2001 *PhD thesis* University of Münster, Germany

- [30] Bratkovskaya E L *et al* 1999 *Eur. Phys. J. A* **4** 165
- [31] Balestra F *et al* 1999 *Phys. Lett. B* **468** 7
- [32] Bratkovskaya E L *et al* 2001 *Preprint nucl-th/0107071 v1*
- [33] Hanhart C and Kudryavtsev A 1999 *Eur. Phys. J. A* **6** 325
- [34] Fäldt G and Wilkin C 1996 *Phys. Lett. B* **382** 209
- [35] Brauksiepe S *et al* 1996 *Nucl. Instrum. Methods A* **376** 397
Moskal P *et al* 2001 *Nucl. Instrum. Methods A* **466** 448 (webpage: <http://ikpe1101.ikp.kfa-juelich.de/>)
- [36] Moskal P *et al* 2002 *Prog. Part. Nucl. Phys.* **49** 1
- [37] Moskal P *et al* 2000 *Phys. Lett. B* **482** 356
- [38] Moskal P *et al* 2000 *Phys. Lett. B* **474** 416
- [39] Falvard A *et al* 1988 *Phys. Rev. D* **38** 2706
- [40] Lockman W S 1989 Talk presented at *3rd Int. Conf. on Hadron Spectroscopy (Ajaccio, France, Sept 23–27) (Ajaccio Hadron)* 1989: 109–118
- [41] Meißner Ulf G and Oller J A 2001 *Nucl. Phys. A* **679** 671
- [42] Kleber V *et al* 2003 *Preprint nucl-ex/0304020*
- [43] Kleber V 2003 *PhD Thesis* Köln University, Germany